Similarity of Quasiconical Shock Wave/Turbulent Boundary-Layer Interactions

Gary S. Settles*
Pennsylvania State University, University Park, Pennsylvania
and
Roger L. Kimmel†
Princeton University, Princeton, New Jersey

A parametric experimental study is reported on the quasiconical shock/boundary-layer interactions produced by three families of shock generators: sharp fins, semicones, and swept compression corners. The experiments were carried out at Mach 2.95 and $Re/m = 6.3 \times 10^7$ using a flat-plate turbulent boundary layer. Over 50 distinct shock generator configurations were considered. The results consist of surface flow patterns, pressure distributions, and flowfield visualizations. An analysis of these results reveals that the interaction characteristics depend primarily on the inviscid shock wave strength and shape. Given similar values of these parameters, "conical free-interaction" similarity results even for disparate shock generators. The similarity conditions among fin, semicone, and swept corner interactions are further explored in terms of normal Mach number scaling and flow regime changes with geometry variation.

Nomenclature

L_i = length along inviscid shock trace to inception of conical flow
M_∞ = incoming freestream Mach number
M_N = component of M_∞ normal to inviscid shock trace or swept leading edge of shock generator
p = surface static pressure, N/m^2
r = local shock wave radius of curvature, cm
Re/m = freestream Reynolds number per meter
$Re\delta$ = Reynolds number based on boundary-layer thickness
x = streamwise distance coordinate, cm
y = vertical distance coordinate normal to flow, cm
z = spanwise (horizontal) distance coordinate normal to flow, cm
α = shock generator angle of attack, deg (Fig. 1)
β = angle of conical interaction feature measured from x axis, deg
β_0 = angle of inviscid shock wave trace in $y=0$ plane measured from x axis, deg
γ = 1.4, ratio of specific heats for air
δ = boundary-layer velocity thickness, cm
Δz = spanwise distance from model apex to conical virtual origin, cm
ζ = shock wave detachment similarity parameter, [Eq. (1)]
λ = shock generator sweepback angle, deg (Fig. 1)
μ = Mach angle, deg
σ = angular difference between β_0 and generator leading edge, deg

Subscripts

C = corner (intersection of shock generator with flat plate)
N = direction normal to inviscid shock trace or swept leading edge
$R1$ = primary reattachment line
SCC = swept compression corner
$S1$ = primary separation line
$S2$ = secondary separation line
U = upstream influence line
∞ = freestream condition

Presented as Paper 84-1557 at the AIAA 17th Fluid Dynamics, Plasma Dynamics, and Lasers Conference, Snowmass, CO, June 25-27, 1984; received Aug. 13, 1984; revision received May 2, 1985.

*Associate Professor of Mechanical Engineering. Member AIAA.
†Graduate Student, Mechanical and Aerospace Engineering Department. Student Member AIAA.

Introduction

THREE-DIMENSIONAL shock wave/turbulent boundary-layer interactions are an important subject in fluid dynamics, considering both their practical significance in supersonic aerodynamics and their current standing as a pacing problem for computational fluid dynamics (CFD). Since the equations of motion for three-dimensional interactions are too complex for significant analytical treatment, most of what we know about them comes from experiments. Such experiments also serve to provide guidance and validation for CFD efforts. The state of understanding of three-dimensional interactions was addressed by Green[1] in 1970 and Peake and Tobak[2] in 1980, and was recently reviewed by Settles and Dolling.[3] Thus, no lengthy literature survey is called for here, other than to point out that past studies of three-dimensional interactions revealed some indications of an overall framework or unifying scheme with which to connect the characteristics of the interactions produced by different shock generators.

The philosophy of past investigators has been to use simple generic shock generator geometries (fins,[4-12] swept steps[13] and compression corners,[14-19] semicones,[20] and transverse cylinders[21-23]) to create swept shocks that interact with otherwise two-dimensional turbulent boundary layers. Despite these attempts at simplification, the resulting interactions were found to be replete with different regimes and subregimes. For example, Zheltovodov[10] found no less than six topologically distinct flow regimes in the sharp fin interaction, which is, at least inviscidly, the simplest of these cases. Similar topological regimes and their boundaries were found for swept compression corner interactions by Settles et al.[15-18]

The next step in the process of understanding three-dimensional interactions calls for a unifying scheme to relate the characteristics of these diverse cases and reduce the magnitude of the problem. Some recent progress has been made in this direction. A scaling law for Reynolds number

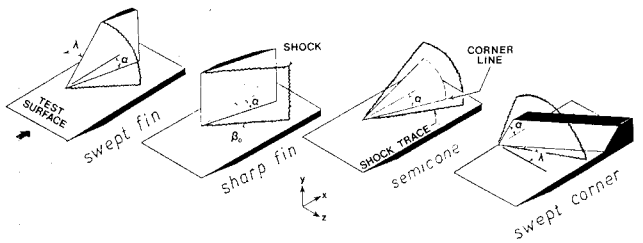

Fig. 1 Conical shock wave generator geometries.

effects was proposed[16] that is effective in correlating both two- and three-dimensional interactions with both turbulent[12,19] and laminar[24] boundary layers. The complete sweepback range of compression corners was studied experimentally[17] and computationally[25] and was found to involve a major regime change from quasicylindrical to quasiconical flow symmetry, along with several subregimes. Most recently, the interactions produced by swept leading-edge fins[26] were found to obey a conical similarity principle based simply on the shape of the inviscid shock wave and not directly upon the fin geometry. However, although progress has been made, an explicit connection between the interactions produced by disparate shock generator geometries has yet to be demonstrated. This is the goal of the present study.

Three families of shock generators are considered: sharp leading-edge fins, swept corners, and semicones (Fig. 1). Parametric experiments were carried out wherein the generator geometry was varied, but the incoming flow conditions ($M_\infty = 2.95$, $Re\delta \simeq 3 \times 10^5$) remained fixed. The aim of this study is to observe the interaction "footprint," or surface topography, as a function of the shock generator geometry; to use the results to discover the flow mechanisms involved; and to find, if possible, a unifying scheme.

Underlying Hypotheses

This study considers only interactions produced by semi-infinite shock generators that impose no length dimension upon the flow. Such generators are known to produce conical flows in purely inviscid supersonic flow, whereas the interactions of such flows with planar boundary layers do not produce purely conical results. Instead, these interactions are asymptotically conical or quasiconical due to the influence of the imposed boundary-layer thickness dimension.

The most available measure of an interaction's characteristics is its topographical "footprint" on the surfaces over which it forms. While footprint topography information is readily obtained by surface flow visualization and pressure techniques, a firm connection between the interaction footprint and the flowfield is nonetheless required.[12,19]

In such an experimental study, careful attention must be paid to the interplay of the deterministic (i.e., inviscid) features of the flow with the vastly more difficult features depending directly upon turbulent transport. The goal of the current research is to gain fundamental new knowledge of the three-dimensional interactions, but not to investigate turbulence physics per se. It follows that the parametric experimental approach adopted here must reach an eventual limit of applicability and that the empirical constants in the resulting similarity rules cannot be explained further until a better understanding of turbulence physics is available.

A further assumption concerns the choice of a coordinate system. Experience dictates that it is easy to go astray with this problem if a poor choice is made.[3] In the present quasiconical case, spherical polar coordinates are called for in principle. In practice, this is approximated with an orthogonal normal-tangential frame, while bearing in mind that the dimensions of conical flow regions are properly expressed only in angular terms. In particular, this normal-tangential frame is based on the *footprint trace of the inviscid shock*, which is the line of interaction of the shock envelope and the test surface in the absence of a boundary layer. The present hypothesis is that the position of the inviscid shock trace is the proper reference position from which to measure the extent of a three-dimensional interaction.

Finally, although the present experiments do not address the issue of flow unsteadiness, it is known to be present to some extent in both two- and three-dimensional shock wave/turbulent boundary-layer interactions.[3] Pending evidence to the contrary, this unsteadiness is assumed not to invalidate the mean flow physical modeling of the interaction process.

Experimental Procedures

Wind Tunnel and Models

The experiments were performed in the Princeton 20×20 cm High Reynolds Number Supersonic Tunnel. A sharp flat plate mounted in the wind tunnel test section provided the interaction test surface, which included several streamwise rows of static pressure taps. The semicone and swept corner models depicted in Fig. 1 were attached to the plate for testing.

Four semicone shock generator models of 15, 20, 25, and 30 deg half-angles were tested. In each case, the semicone axis was aligned with the freestream direction. The swept compression corner test matrix consisted of 20 different combinations of the defining angles α and λ as shown in Fig. 2. Some of the data in this test matrix were already available from previous experiments.[15-19] The details of model configurations, mounting, aerodynamic fences, and pressure tap locations are given in the references cited. A special series of rhombic cone models was tested in inviscid flow along the tunnel centerline in order to provide data for the correlation of inviscid shock angles described later.

No fin shock generators were tested specifically for the current study. Instead, the $\alpha = 9$ and 15 deg swept fin results of Lu and Settles[26] were used, along with a collection of unswept fin data[7,28] obtained under identical conditions in the same facility with $4 \leq \alpha \leq 20$ deg.

Test Conditions

The experiments were conducted at $M_\infty = 2.95$ with a stagnation temperature of 261 K $\pm 4\%$, a stagnation pressure of 0.689×10^6 N/m^2, and a nominal freestream Reynolds number of 6.3×10^7/m. A fully developed, two-dimensional, approximately adiabatic, turbulent boundary layer having a zero pressure gradient was developed on the flat plate. This boundary layer met the usual wall-wake law criterion for mean flow equilibrium. The overall (velocity) thickness, displacement, and momentum thicknesses of the boundary layer approaching the interaction location (25 cm from the plate leading edge) were 0.39, 0.112, and 0.023 cm, respectively, and $c_f = 1.43 \times 10^{-3}$. Note, however, that the boundary-layer thickness grew with the distance along the plate, reaching a value of 0.5 cm or more at the downstream boundary of the testing region.

Techniques and Instrumentation

As mentioned earlier, the present experiments consider mainly the mean "footprints" of conical interactions as revealed by surface flow visualization and static pressure measurements. The surface flow patterns were obtained by a specialized kerosene/lampblack streak technique[27] and surface pressures were read from taps in the flat plate connected to a scanivalve. Extensive comparisons of these results have shown that they give equivalent indications of upstream influence in shock wave/boundary-layer interactions. In addition to these measurements, a localized vapor-screen technique[27] was used to visualize boundary layer flow separation. Also, direct shadowgraphy was used to measure inviscid shock shapes as described next.

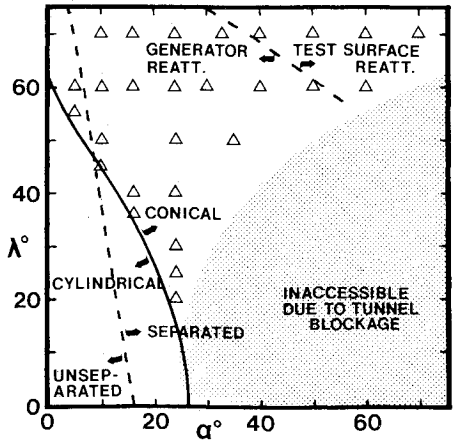

Fig. 2 Swept corner test matrix showing regime boundaries ($M_\infty = 2.95$).

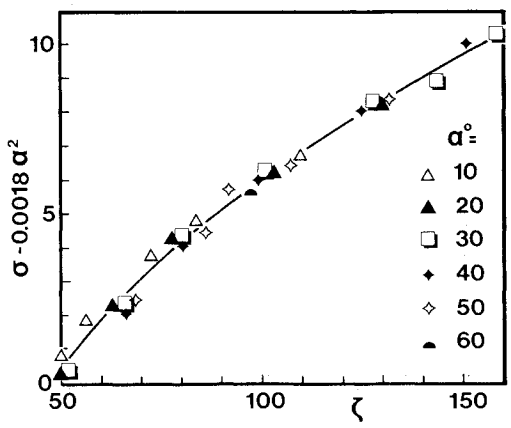

Fig. 3 Shock detachment angle correlation for swept corners ($M_\infty = 2.95$).

Results and Discussion

Inviscid Flows and Shock Shapes

According to the earlier discussion of coordinate frames, a knowledge of the position of the inviscid shock trace in the plane of the flat plate is required. This can be specified by a single angle, β_0, as shown in Fig. 1. However, determining β_0 is not trivial. It is known a priori only for unswept fins (from the exact oblique shock theory) and for semicones (from the Taylor-MacColl theory). For swept fins and compression corners, no simple solutions exist and the determination of the shock shape requires either a shock-fitting computational Euler solver or else a series of experiments. These experiments involved the measurement of a wide range of shock shapes directly from shadowgrams of the flow over rhombic cones and delta wings at angles of attack.[26]

The rhombic cone experiments were designed to cover the α,λ range of the swept compression corner interactions of current interest, namely, $20 \le \alpha \le 70$ and $5 \le \lambda \le 70$ deg, which encompass the majority of the practical ranges of conical interactions at Mach 2.95 (see Fig. 2). The results of this set of experiments may be expressed as a correlation of the angle $\sigma = \beta_0 + \lambda - 90$ deg as shown in Fig. 3. The abscissa of Fig. 3 is a *detachment similarity parameter* derived from a second-order polynomial curve fit of the expression for the maximum stream deflection by a wedge in oblique shock theory,

$$\zeta = (\alpha_N + 38.53)/[M_N(1 - 0.149M_N)] \qquad (1)$$

where ζ has a constant value of 43.6 for shock detachment from swept wedges at supersonic Mach numbers up to 3 and

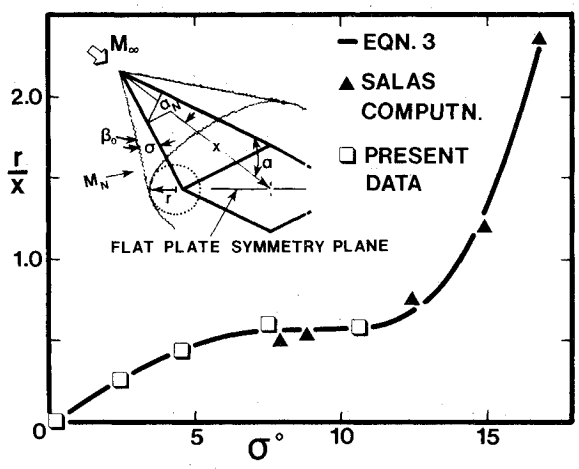

Fig. 4 Local shock radius vs detachment angle ($M_\infty = 2.95$).

α_N and M_N are the corner angle in degrees and Mach number component in the direction normal to the model leading edge, respectively.

The correlation of Fig. 3 is valid for $\alpha \le 50$ deg and, noting that $M_N = 2.95\cos\lambda$, can be expressed solely in terms of shock generator geometry by

$$\sigma = -6.85 + 0.1\arctan^2(0.339M_N\tan\alpha_N) + 0.168\zeta - 0.000385\zeta^2 \qquad (2)$$

This correlation matches the original shadowgram data to within ± 0.5 deg over its range of validity. It not only provides the desired values of β_0 for the interaction analysis, but also has some intrinsic value of its own, since very few previous results have been published concerning the inviscid flow over swept corners with conically detached shocks.[29,30]

For later use, it is important to know not only the inviscid shock angle β_0, but also the shape of the shock in the vicinity of the swept corner. Prior to detachment, the shock is, of course, planar. Beyond detachment, one can make a first approximation that the shock follows some circular arc in the corner vicinity, by analogy with previous studies of two-dimensional detachment from wedges. The problem is then to find the variation of the local shock radius of curvature with the detachment distance, recognizing that in the present quasiconical flow both quantities must be dimensionless. An appropriate form for the conical shock radius is r/x, while an appropriate form for the detachment "distance" is simply σ (the angle between a swept corner and its corresponding shock in the flat-plate plane of symmetry).

By taking shadowgrams of several rhombic cone models at various roll angles, it was possible to plot the corresponding shock shapes and thus obtain several r/x vs σ data points. Salas[29] has also computed and published the shock shapes for five swept corner cases at Mach 3. The combined results for r/x vs σ are shown in Fig. 4, revealing that the shock radius grows rapidly following detachment, then more slowly, and then rapidly again as the shock moves well away from the corner. The curve of r/x vs σ thus has an inflection at about $r/x = 0.55$. The polynomial fit shown in Fig. 3 has the equation

$$r/x = -0.0108 + 0.0879\sigma + 0.0126\sigma^2 - 0.00305\sigma^3 + 0.000146\sigma^4 \qquad (3)$$

which allows r/x to be expressed purely in terms of the shock generator defining parameters α_N and M_N through Eq. (2).

Values of r/x for the swept fins were obtained in a similar way from the shadowgrams of Lu[26,31] and were checked against the approximate analytical method of Roe[32] for flat delta wing shock shapes. Note that $r/x \to \infty$ as $\lambda \to 0$ for fin-

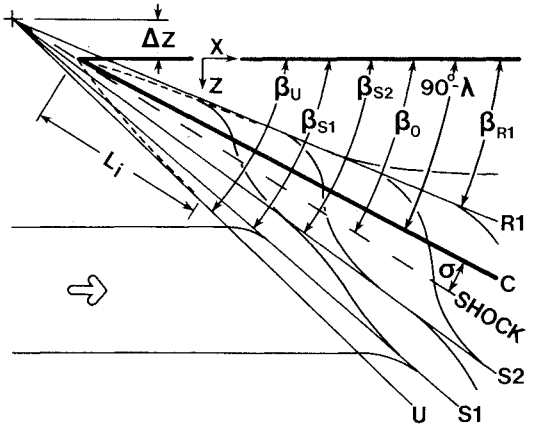

Fig. 5 Typical interaction surface streakline topography.

generated shock waves. Semicone shock r/x values are simply equal to $\tan\beta_0$.

Interaction Characteristics

A schematic of the surface streakline topography of a swept corner interaction is shown in Fig. 5 for purposes of illustration. Such patterns have been described fully by Settles and Teng,[17] including proof of conical symmetry by way of similarity of surface pressure distributions in normalized spherical coordinates. Here, it suffices to point out the initial nonconical inception zone of length L_i which is followed in the spanwise direction by conical symmetry. In this conical region, the lines circumscribing the surface topography (denoted by the angles β_U, β_{S1}, and β_{S2}) are straight and convergent upon a conical virtual origin. The inviscid shock angle β_0 and the angle σ are also shown. Note that, aside from L_i, the entire interaction footprint is inherently dimensionless.

Figure 5 is meant to illustrate a generic quasiconical interaction that might be produced by any of the three shock generators considered here. However, there are some subtle distinctions. Figure 5 shows both the primary and secondary separation lines, although a small minority of fin and swept corner interactions show no evidence of boundary-layer separation (note the incipient primary separation boundary for swept corner interactions in Fig. 2). In all cases where the secondary separation phenomenon was present, it appeared to be near incipient conditions, such that the secondary separation and reattachment lines ($S2$ and $R2$) were essentially coincident. Most important, the primary reattachment line $R1$ is shown in Fig. 5 to lie on the shock generator rather than on the test surface, although this was not always the case.

For all separated fin interactions observed in this study and those with which the authors are familiar, primary reattachment always occurs on the test surface and never on the shock generator itself. In contrast, the semicone interactions observed here and those of Avduyevskii and Gretsov[20] always produced reattachment on the shock generator. The same was true of the majority of present swept corner interactions except for five extreme cases: $(\alpha,\lambda)=(60,60)$, (40,70), (50,70), (60,70), and (70,70), in which R1 was found on the test surface. The phenomenon of the flow regime boundary between the reattachments based on the test surface and the generator is discussed further in the next section.

Figure 6 shows flowfield visualization photos of the boundary-layer separation regions produced by typical fin, semicone, and swept corner models. These photographs were obtained by the local vapor-screen method of Settles and Teng[27] with the light sheet oriented normal to the test surface and approximately normal to the inviscid shock wave as well. For the cases shown, reattachment occurs on the semicone and swept corner shock generators, but lies on the test

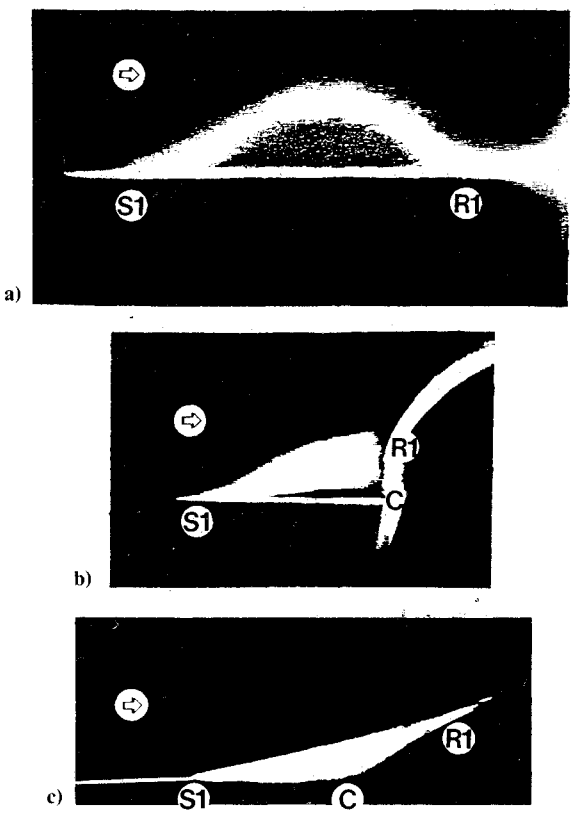

Fig. 6 Vapor screen visualizations of flow separation due to a) $\alpha=15$ deg unswept fin, b) $\alpha=30$ deg semicone, and c) $\alpha=24$ deg, $\lambda=40$ deg swept corner.

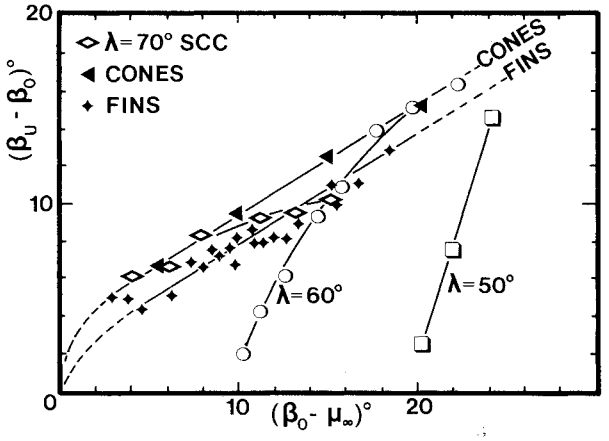

Fig. 7 Interaction response $(\beta_U-\beta_0)$ vs shock angle $(\beta_0-\mu_\infty)$.

surface for the fin interaction as described above. The interpretation of these photos was supported by extensive direct observations and videotaped flow visualization results.

Interaction Similarity Conditions

In order to consider the conditions under which quasiconical interactions exhibit similarity, one must begin with an appropriate choice of dependent and independent variables. Suitable candidates for the dependent "interaction response function" are the included angle of the separation zone $(\beta_{S1}-\beta_{R1})$ or the angular difference between the inviscid shock trace and the upstream influence line $(\beta_U-\beta_0)$. The "strength" of the inviscid shock is given to a first approximation by $(\beta_0-\mu_\infty)$. The latter two parameters are plotted as the ordinate and abscissa, respectively, in Fig. 7.

Both the semicone and fin results lie approximately along straight lines in Fig. 7, indicating that the interaction response or growth is a linear function of the inviscid shock

angle. However, this function is slightly different for the two shock generators:

$$\beta_U = 1.59\beta_0 - 8.3 \quad \text{(semicones, } M_\infty = 2.95\text{)} \tag{4}$$

$$\beta_U = 1.59\beta_0 - 10.0 \quad \text{(fins, } M_\infty = 2.95\text{)} \tag{5}$$

While both lines have the same slope, they have different intercepts and neither passes through the origin. The difference in intercept may be attributable to the fact that the shapes of flow separation regions produced by fins and semicones are different (Fig. 6), while the fact the intercepts are nonzero clearly indicates that the growth rate of very weak interactions [$(\beta_0 - \mu_\infty) \leq 4$ deg] is nonlinear.[33] In any case, Fig. 7 reveals a limited form of conical similarity for semicone and fin interactions. (Note, as in Ref. 26, that the fin interactions described by Eq. (5) are produced by geometrically dissimilar shock generators having a wide range of leading-edge sweep angles.) However, no such similarity is evident in Fig. 7 for swept corner interactions.

In retrospect, a simple collapse of the swept corner data in the coordinates of Fig. 7 is not expected. While the inviscid flowfields of both the fin and semicone interactions have inherently moderate-to-high values of shock standoff angle σ and shock radius r/x, these parameters are generally smaller for swept corner interactions. (In fact, both σ and r/x are zero at the shock detachment from a swept corner, which marks the lower bound of the conical interaction regime.[17]) One should then expect the shock curvature r/x to play an important part in the comparison of swept corner interactions.

On the other hand, the swept corner interaction response cannot be purely a function of shock r/x. The two degrees of freedom, α and λ, in the shock generator geometry allow the same shock radius to occur at different sweepback angles. The more highly swept the interaction is for a given shock radius, the lower will be the values of M_N and the corresponding maximum pressure ratio across the shock. As expected, a reduced shock pressure ratio leads to a reduction in interaction response at high sweep angles.

In order to take this into account, the interaction response function requires normalization by a third parameter expressing the shock pressure ratio as a function of the sweepback angle. Note that the inviscid shock must meet the test surface at a normal angle regardless of the shock curvature, provided the shock is detached from the swept corner. The maximum pressure ratio across this swept normal shock is given by the exact oblique shock theory as

$$\frac{p_2}{p_1} = \left(\frac{2\gamma}{\gamma+1}\right) M_N^2 - \frac{\gamma-1}{\gamma+1}$$

$$= 1.66 M_N^2 - 0.66 \text{ for air} \tag{6}$$

For simplification this can be written $p_2/p_1 = 1.16\ M_N^2$ with acceptable error for $1 \leq M_N \leq 3$. We may thus use M_N^2 as a straightforward shock strength normalizer of the interaction response function, although bearing in mind that the interaction actually splits the shock wave into a "lambda foot,"[11,27] so the overall pressure ratio $p_2/p_1 \sim M_N^2$ may be regarded as a reference condition for the inviscid shock strength.

The results are shown in Fig. 8, which is a similarity plot of $(\beta_{S1} - \beta_{R1})/M_N^2$ vs r/x. The normalized interaction response function is well correlated in this form for swept corners over the entire present range of the corner defining parameters α and λ. Further, the response function grows linearly with r/x according to

$$(\beta_{S1} - \beta_{R1})/M_N^2 = 13.7\,(r/x) + 1 \quad \text{(swept corners, } M_\infty = 2.95\text{)} \tag{7}$$

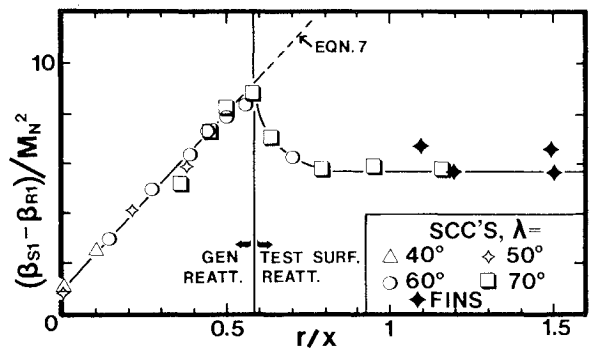

Fig. 8 Interaction response $(\beta_{S1} - \beta_{R1})/M_N^2$ vs shock radius r/x.

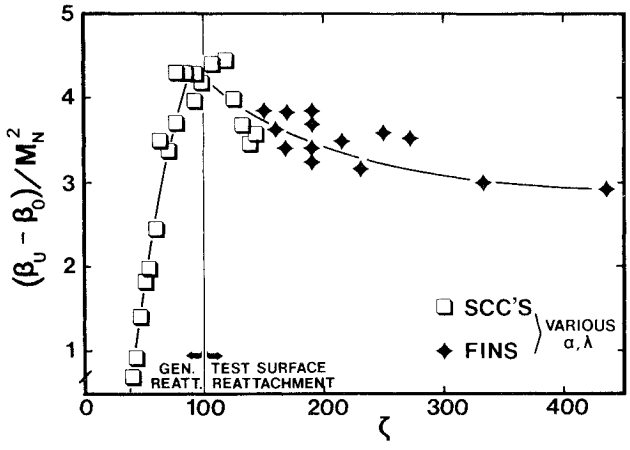

Fig. 9 Interaction response $(\beta_U - \beta_0)/M_N^2$ vs detachment similarity parameter ζ.

up to a critical value of $r/x = 0.58$, whereupon it decreases and then tends toward a constant value with any further increase in r/x.

The significance of the critical value $r/x = 0.58$ is that it marks the rapid migration of the flow reattachment line $R1$ from the swept corner generator surface to the test surface. This phenomenon was observed for the two most highly swept corner families ($\lambda = 60$ and 70 deg) and is exactly correlated for both in Fig. 8. For $r/x > 0.58$, the swept corner interactions become topographically similar to swept fin interactions, also represented in the figure.

The same similarity behavior is shown in Fig. 9, where the $(\beta_U - \beta_0)/M_N^2$ response function is plotted against the detachment similarity parameter. The latter choice was made in order to show more of the available fin data, since ζ and r/x are related by Eqs. (1-3), but ζ does not tend toward infinity for planar shocks as does r/x. The swept and unswept fin results shown in Fig. 9 cover the range $6 \leq \alpha \leq 20$ deg. Figures 8 and 9 also demonstrate that the choice of which conical feature angles one uses to form the interaction response function is not critical to the similarity result.

The semicone data, not shown in Figs. 8 and 9, do not reveal a flow regime change at $r/x = 0.58$. Since semicone shock generators do not belong to the same geometrical family as swept corners and fins, the conditions that force reattachment off the generator and onto the test surface in the latter family are not expected to hold for semicones. Further research is required to find a geometrical transformation with which the reattachment conditions on semicone and swept corner shock generators can be compared properly.

In summary, the similarity of fin- and swept corner-generated interactions can be written in simple functional form as

$$\Delta\beta/M_N^2 = f_1(r/x) = f_2(\zeta) \qquad (M_\infty = 2.95) \tag{8}$$

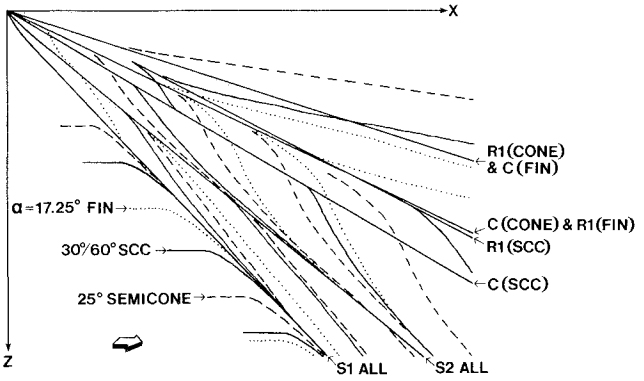

Fig. 10 Comparison of streakline patterns of similar fin, semicone and swept compression corner (SCC) interactions.

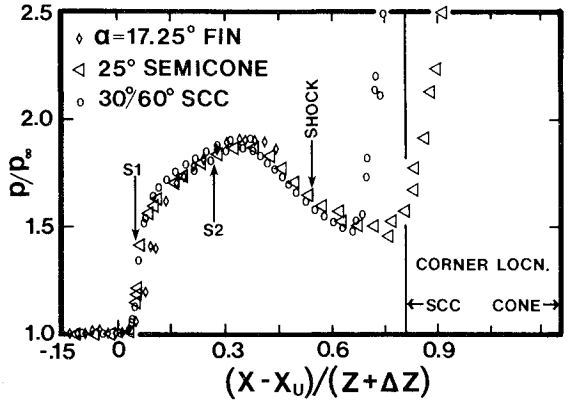

Fig. 11 Free interaction surface pressure comparison.

where $\Delta\beta$ represents a general interaction response function and f_1, f_2 represent the shapes of the curves shown in Fig. 8 and 9, respectively.

Conical "Free Interaction"

It was found by examination of the present data that, under the proper conditions, the surface streakline pattern of one interaction can be found to match that of another almost exactly, even though the two patterns were produced by dissimilar shock generators. The conditions for this to occur require that the inviscid shock angle and local shock radius of curvature be similar for the interactions being compared, so that both β_0 and β_U are approximately matched. (Note that points which lie in close proximity in Fig. 7 satisfy these conditions automatically.) Such is the case for any fin and semicone interactions having the same β_0 per Eqs. (4) and (5). However, restrictions are placed on r/x for swept compression corner interactions, since these may occur at different strengths for the same value of β_0. If r/x is large it has little effect, but it has a definite effect when its value is of order one or less.

An example of this pattern similarity is shown in Fig. 10. The streakline patterns of the 25 deg semicone and $(\alpha,\lambda)=(30,60)$ deg swept corner interactions are compared in overlay with that of an unswept fin with $\alpha=17.25$ deg.[28] These three cases have $\beta_0=35.1$ deg $\pm 1\%$ and $\beta_U=46.6$ deg ± 1.5 %. Their surface topography is strikingly similar, despite major differences in the shock generator geometry and despite the fact that two different flow reattachment regimes are represented. Equally good comparisons were found between the 15 deg semicone and (16,70) deg corner, the 30 deg semicone and (50,60) deg corner, and the 15 deg unswept fin and (50,70) corner interactions. In general, the agreement is best near the beginning of the interaction and deteriorates as the generator/test surface junction is approached.

This fact is also seen in the comparison of surface pressure distributions shown in Fig. 11 for the three interactions whose footprints are compared in Fig. 10. The abscissa of Fig. 11 is scaled such that the beginning of the pressure rise is coincident for each of the three cases and the differences in the span have been taken into account by normalizing by the spanwise distance from the conical virtual origin, $z+\Delta z$. The three distributions are in excellent agreement at least as far as the pressure plateau, but a divergence of the semicone and swept corner data is obvious further downstream. (The fin pressure data were read only up to the plateau.[28])

This is highly reminiscent of the two-dimensional "free interaction" concept first proposed by Chapman et al.[34] Their idea that certain shock/boundary-layer interactions have initial regions dependent only on incoming and not downstream conditions has been supported by many experiments since it was originally suggested in 1957. Indications of three-dimensional free interaction similarity have also been found by Soviet investigators.[35,36] Note that the primary requirement for a free interaction—that there be significant boundary-layer separation—is satisfied by most of the present quasiconical interactions.

Conclusions

A parametric experimental study has been made of the quasiconical shock boundary-layer interactions produced by three families of shock generators: sharp fins, semicones, and swept compression corners. The experiments were carried out at Mach 2.95 and $Re/m=6.3\times10^7$ using a flat-plate turbulent boundary layer. Over 50 distinct shock generator configurations were considered. The results consist of surface flow patterns, pressure distributions, and flowfield visualizations. An analysis of these results leads to the following conclusions:

1) The interaction characteristics depend primarily upon the inviscid shock wave strength and shape. When characterized by an overall angular "interaction response function," the flows studied here were correlated by simple dependencies on inviscid shock angle, normal Mach number, and local shock radius of curvature.

2) A similarity rule for inviscid conical shock detachment angles from swept compression corners was developed as a necessary early step in comparing swept corner interactions with those produced by other shock generators.

3) Most of the interactions considered involved extensive quasiconical regions of boundary-layer separation, as revealed by both surface streak patterns and flowfield visualizations.

4) A significant flow regime boundary for swept corner interactions was identified with the position of the flow reattachment line, whether on the shock generator or on the test surface.

5) An explicit connection was found between swept corner- and fin-generated interactions, in which the reattachment flow regime boundary plays a critical role.

6) Scaling of the interaction response by the shock strength (M_N^2) was found to be a necessary condition for the comparison of similar interactions produced by geometrically dissimilar shock generators.

7) A conical "free interaction" principle similar to that for two-dimensional flows was found. Given similar values of shock and upstream influence angles, the footprint topography of fin, semicone, and swept corner interactions was found to be virtually identical. Surface pressure similarity was also demonstrated.

8) The disparity in flow reattachment conditions for semicone shock generators compared to that for fins and swept corners requires further study.

Acknowledgments

This study was carried out under AFOSR Contract F49620-81-K-0018 with Princeton University and a related

subcontract with Pennsylvania State University, monitored by Dr. James D. Wilson. The authors are grateful to Profs. S. M. Bogdonoff and D. S. Dolling, Dr. C. C. Horstman, and Mr. S.-Y. Wang for helpful comments.

References

[1]Green, J. E., "Interaction Between Shock Waves and Boundary Layers," *Progress in Aerospace Sciences*, Vol. 11, Pergamon Press, New York, 1970, pp. 235-340.

[2]Peake, D. J. and Tobak, M., "Three-Dimensional Interactions and Vortical Flows with Emphasis on High Speeds," NASA TM 81169, March 1980.

[3]Settles, G. S. and Dolling, D. S., "Swept Shock Wave/Boundary Layer Interactions," *AIAA Progress in Astronautics and Aeronautics: Tactical Missile Aerodynamics*, edited by J. Nielsen and M. Hemsch, AIAA, New York, 1986, to be published.

[4]Stanbrook, A., "An Experimental Study of the Glancing Interaction Between a Shock Wave and a Boundary Layer," British ARC-CP-555, July 1960.

[5]McCabe, A., "A Study of Three-Dimensional Interactions Between Shock Waves and Turbulent Boundary Layers," Ph.D. Thesis, Univ. of Manchester, England, Oct. 1963.

[6]Lowrie, B. W., "Cross-Flow Produced by the Interaction of a Swept Shock Wave with a Turbulent Boundary Layer," Ph.D. Thesis, Cambridge Univ., England, 1965.

[7]Oskam, B., Vas, I. E., and Bogdonoff, S. M., "Mach 3 Oblique Shock Wave/Turbulent Boundary Layer Interactions in Three Dimensions," AIAA Paper 76-336, July 1976.

[8]Peake, D. J., "The Three-Dimensional Interaction of a Swept Shock Wave with a Turbulent Boundary Layer and the Effects of Air Injection on Separation," Ph.D. Thesis, Carleton Univ., Ottawa, Canada, March 1975.

[9]Zheltovodov, A. A., "Properties of Two- and Three-Dimensional Separation Flows at Supersonic Velocities," *Izvestiya Akademii Nauk SSSR, Mekhanika Zhidkosti i Gaza*, No. 3, May-June 1979, pp. 42-50.

[10]Zheltovodov, A. A., "Regimes and Properties of Three-Dimensional Separation Flows Initiated by Skewed Compression Shocks," *Zhurnal Prikladnoi Mekhaniki i Tekhnicheskoi Fiziki*, No. 3, May-June 1982, pp. 116-123.

[11]Zubin, M. A. and Ostapenko, N. A., "Structure of Flow in the Separation Region Resulting from Interaction of a Normal Shock Wave with a Boundary Layer in a Corner," *Izvestiya Akademii Nauk SSSR, Mekhanika Zhidkosti i Gaza*, No. 3, May-June 1979, pp. 51-58.

[12]McClure, W. B. and Dolling, D. S., "Flowfield Scaling in Sharp Fin-Induced Shock Wave Turbulent Boundary Layer Interaction," AIAA Paper 83-1754, July 1983.

[13]Stalker, R. J., "Sweepback Effects in Turbulent Boundary-Layer Shock-Wave Interaction," *Journal of the Aeronautical Sciences*, Vol. 27, May 1960, pp. 348-356.

[14]Bachalo, W. D., "Three-Dimensional Boundary Layer Separation in Supersonic Flow," Univ. of California, Berkeley, Rept. FM-74-10, Aug. 1974.

[15]Settles, G. S., Perkins, J. J., and Bogdonoff, S. M., "Investigation of Three-Dimensional Shock/Boundary Layer Interactions at Swept Compression Corners," *AIAA Journal*, Vol. 18, July 1980, pp. 779-785.

[16]Settles, G. S. and Bogdonoff, S. M., "Scaling of Two- and Three-Dimensional Shock/Turbulent Boundary Layer Interactions at Compression Corners," *AIAA Journal*, Vol. 20, June 1982, pp. 782-789. (cf., AIAA Paper 81-0334, Jan. 1981.)

[17]Settles, G. S. and Teng, H.-Y., "Cylindrical and Conical Flow Regimes of Three-Dimensional Shock/Boundary Layer Interactions," *AIAA Journal*, Vol. 22, Feb. 1984, pp. 194-200.

[18]Settles, G. S. and Teng, H.-Y., "A Test of the Independence Principle in Swept Cylindrical Shock Wave/Turbulent Boundary Layer Interactions," Paper presented at 2nd Asian Congress of Fluid Mechanics, Beijing, China, Oct. 1983.

[19]Settles, G. S., Horstman, C. C., and McKenzie, T. M., "Flowfield Scaling of a Swept Compression Corner Interaction—A Comparison of Experiment and Computation," AIAA Paper 84-0096, Jan. 1984; also *AIAA Journal*, to be published.

[20]Avduyevskii, V. S. and Gretsov, V. K., "Investigation of the Three-Dimensional Separation Flow Around Semicones on a Flat Plate," *Izvestiya Akademii Nauk SSSR, Mekhanika Zhidkosti i Gaza*, No. 6, Nov.-Dec. 1970, pp. 112-115.

[21]Westkaemper, J. C., "Turbulent Boundary Layer Separation Ahead of Cylinders," *AIAA Journal*, Vol. 6, July 1968, pp. 1352-1355.

[22]Dolling, D. S., "Comparison of Sharp and Blunt Fin-Induced Shock Wave/Turbulent Boundary-Layer Interaction," *AIAA Journal*, Vol. 20, Oct. 1982, pp. 1385-1391.

[23]Dolling, D. S. and Bogdonoff, S. M., "Blunt Fin-Induced Shock Wave/Turbulent Boundary-Layer Interaction," *AIAA Journal*, Vol. 20, Dec. 1982, pp. 1674-1680.

[24]Degrez, G. and Ginoux, J. J., "Surface Phenomena in a Three-Dimensional Skewed Shock Wave/Laminar Boundary Layer Interaction," *AIAA Journal*, Vol. 22, Dec. 1984, pp. 1764-1769.

[25]Horstman, C. C., "A Computational Study of Complex Three-Dimensional Compressible Turbulent Flow Fields," AIAA Paper 84-1556, June 1984.

[26]Settles, G. S. and Lu, F. K., "Conical Similarity of Shock/Boundary Layer Interactions Generated by Swept and Unswept Fins," *AIAA Journal*, Vol. 23, July 1985, pp. 1021-1027.

[27]Settles, G. S. and Teng, H.-Y., "Flow Visualization Methods for Separated Three-Dimensional Shock Wave/Turbulent Boundary Layer Interactions," *AIAA Journal*, Vol. 21, March 1983, pp. 390-397.

[28]Goodwin, S. P., "An Exploratory Investigation of Sharp Fin-Induced Shock Wave/Turbulent Boundary Layer Interactions at High Shock Strengths," M.S.E. Thesis 1687-T, Princeton Univ., Princeton, NJ, Nov. 1984.

[29]Salas, M. D., "A Careful Numerical Study of Flowfields About External Conical Corners: Part I—Symmetric Configurations," AIAA Paper 79-1511, July 1979.

[30]Bannink, W. J., "Investigation of the Conical Flowfield Around External Axial Corners," *AIAA Journal*, Vol. 22, March 1984, pp. 354-360.

[31]Lu, F. K., "An Experimental Study of Three-Dimensional Shock Wave/Boundary Layer Interactions Generated by Sharp Fins," M.S.E. Thesis, Princeton Univ., Princeton, NJ, Rept. MAE 1584-T, March 1983.

[32]Roe, P. L., "A Simple Treatment of the Attached Shock Layer on a Delta Wing," British RAE TR 70246, Dec. 1970.

[33]Dolling, D. S., "Upstream Influence in Conically Symmetric Flow," *AIAA Journal*, Vol. 23, June 1985, pp. 967-969.

[34]Chapman, D. R., Kuehn, D. M., and Larson, H. K., "Investigation of Separated Flows in Supersonic and Subsonic Streams with Emphasis on the Effect of Transition," NACA TN 3869, March 1957.

[35]Panov, Y. A., "Interaction of Incident Three-Dimensional Shock with a Turbulent Boundary Layer," *Fluid Dynamics*, Vol. 3, May-June 1968, pp. 108-110.

[36]Avduyevskii, V. S. and Medvedev, K. I., "Effect of Three-Dimensional Flow on Limiting Pressure Differential for Interaction of Boundary Layer with Shock Waves," *Fluid Dynamics*, Vol. 2, March-April 1967, pp. 32-34.